computation

MDPI

Article

Optimization of the Small Wind Turbine Design—Performance Analysis

Marek Jaszczur [1], Marek Borowski [2], Joanna Halibart [2,*], Klaudia Zwolińska-Glądys [2,*] and Patryk Marczak [1]

[1] Faculty of Energy and Fuels, AGH University of Krakow, al. Adama Mickiewicza 30, 30-059 Kraków, Poland; jaszczur@agh.edu.pl (M.J.); pmarczak@agh.edu.pl (P.M.)
[2] Faculty of Civil Engineering and Resource Management, AGH University of Krakow, al. Adama Mickiewicza 30, 30-059 Kraków, Poland; borowski@agh.edu.pl
* Correspondence: jhalibart@gmail.com (J.H.); kzwolinska@agh.edu.pl (K.Z.-G.)

Abstract: In recent decades, the intensive development of renewable energy technology has been observed as a great alternative to conventional energy sources. Solutions aimed at individual customers, which can be used directly in places where electricity is required, are of particular interest. Small wind turbines pose a special challenge because their design must be adapted to environmental conditions, including low wind speed or variability in its direction. The research study presented in this paper considers the energy efficiency of a small wind turbine with a horizontal axis of rotation. Three key design parameters were analyzed: the shape and inclination of the turbine blades and additional confusor–diffuser shape casings. The tests were carried out for three conceptual variants: a confusor before the turbine, a diffuser after the turbine, and a confusor–diffuser combination. Studies have shown that changing the shape of the blade can increase the analyzed wind turbine power by up to 35%, while changing the blade inclination can cause an increase of up to 16% compared to the initial installation position and a 66% increase in power when comparing the extreme inclination of the blades of the tested turbine. The study has shown that to increase the wind speed, the best solution is to use a confusor–diffuser configuration, which, with increased length, can increase the air velocity by up to 21%.

Keywords: small wind turbine; horizontal-axis wind turbine; diffuser/confusor augmented wind turbine; wind concentrators; computational fluid dynamics

Citation: Jaszczur, M.; Borowski, M.; Halibart, J.; Zwolińska-Glądys, K.; Marczak, P. Optimization of the Small Wind Turbine Design—Performance Analysis. *Computation* **2024**, *12*, 215. https://doi.org/10.3390/computation12110215

Academic Editors: Ali Cemal Benim, Abdulmajeed A. Mohamad, Sang-Ho Suh, Rachid Bennacer, Paweł Oclon and Jan Taler

Received: 1 September 2024
Revised: 16 October 2024
Accepted: 21 October 2024
Published: 25 October 2024

1. Introduction

The increase in greenhouse gas emissions, high energy consumption, and depletion of natural resources are just some crucial factors that contribute to the development of alternative-energy-source technologies. Renewable energy is a fundamental element of the sustainable energy strategy. Due to its inexhaustible potential, its affordability, the reduction in pollution, and the availability of new technologies on the market, renewable energy sources are an interesting alternative to generating energy based on fossil fuels. Among the solutions commonly used and available on the market, there are photovoltaic panels, wind turbines, and hydroelectric power plants. In recent years, wind power plants have gained popularity. Wind potential has long been widely used by humans in everyday life, initially in navigation and as a driving force for windmills used in pumping water systems or mills. Currently, many solutions are available on the market, differing in construction, electrical power, and turbine size.

1.1. Wind Energy

Wind energy has become one of the most dynamically developing industries in recent years. Extensive wind farms are a common element of the landscape of many countries. In addition, more and more wind turbines are being installed on the roofs of buildings or

nearby. The wind turbine is the most important element of every wind power plant that converts the kinetic energy of the wind into useful electrical energy. The design parameters of the turbine determine the properties and power achieved by the wind power plant.

Depending on the position of the axis of rotation of the turbine rotor, Horizontal-Axis Wind Turbines (HAWT) and Vertical-Axis Wind Turbines (VAWT) turbines are distinguished. Currently, the most commonly used solution involves large wind turbine sets with a horizontal axis, where the height can reach a height of up to 100 m. The production of wind power plants depends on the design of the wind turbines and the wind speed. Turbines with a vertical axis of rotation are increasingly being used in urbanized areas, where they are installed directly on buildings. The blades of this design generate less noise, and their main advantage is their independence from changes in the wind direction, as they do not require the use of mechanisms for setting up against the wind direction, unlike turbines with a horizontal axis. This type of construction could operate at low values of wind velocity and is characterized by a simple, easy-to-maintain structure [1].

1.2. Energy Efficiency of Wind Turbines

Wind energy is a widely available source of energy that can be effectively converted into electrical energy using appropriate technologies. Existing mathematical formulas allow the estimation of the electrical power that could be obtained from the operating wind turbine. This formula presents the relationships of the amount of generated energy that can be obtained from the wind under a given wind speed, dependent on the device efficiency resulting from the turbine design. The value of the power P generated from the wind can be estimated from the following formula [2]:

$$P = C_p \cdot \frac{\rho}{2} \cdot A \cdot {v_w}^3 \quad (1)$$

where ρ is the air density (kg/m^3), v_w is the air velocity (m/s), A defines the swept area of the blades (m^2), and C_p denotes the power coefficient.

This equation shows the importance of the wind velocity, which is in the third power. Wind speed is the main factor taken into account in the analysis of wind energy. Doubling the wind speed causes an eight-fold increase in the wind turbine power. The power of the wind turbine also depends on the area swept by the turbine blades, which signifies the advantages of large wind turbine blades. The formula also includes the power coefficient C_p, which expresses the degree of utilization of the total wind power. According to Betz's theory, the maximum possible value of C_p is approximately 59% [3]. The power coefficient depends on the type of wind turbine and changes for a given design, depending on the tip speed ratio (TSR), which expresses the ratio of the velocity of the blade tip to the wind speed [2]. Figure 1 presents the power coefficient C_p values for different wind turbine solutions and the different values of the tip speed ratio (TSR).

1.3. Optimization Solutions to Increase the Efficiency of Wind Turbines

Commercial wind turbines are currently made mostly with a horizontal axis of rotation and with three blades. They constitute about 95% of all installed turbines [4]. A small percentage of the market is covered with wind turbines with a vertical axis of rotation. Currently offered devices are mostly large structures, typically designed and optimized as free-standing devices. Very often, designers or constructors do not consider interactions of the wind turbine with the surrounding constructions. The widespread increased interest in distributed energy is a contribution to scientists' attention to small wind turbines intended for individual purposes. One of the main limitations in domestic application is the low wind speed and high turbulence intensity caused by the roughness of the terrain and existing buildings. An additional challenge is the prediction of the actual efficiency of small wind turbines due to the difficulties in estimating wind conditions in a given location without having detailed measurements [5]. For this reason, research in this area mainly focuses on optimizing the structures used to improve their efficiency in unfavorable conditions.

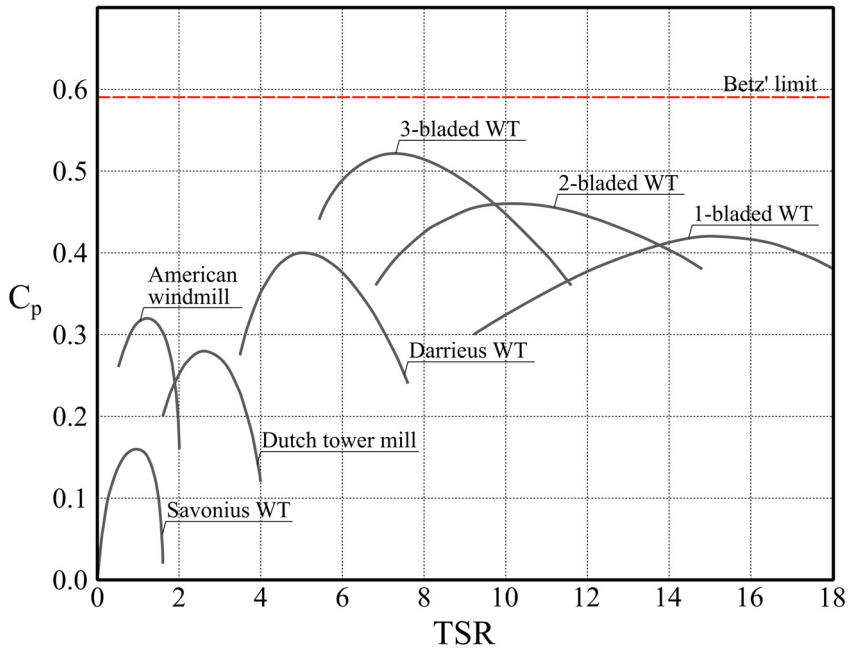

Figure 1. Dependence of the power coefficient C_p on the TSR for different types of wind turbines. Based on [1].

In the literature, several analyses of the shape of blades or rotors and their impact on the obtained power can be found [6–11]. At the design step, it is necessary to consider not only the maximization of efficiency and minimization of the costs of obtained electric energy, but also operational problems such as the start-up velocity and the low wind speed at which the turbine should also operate [10]. Rezaeiha et al. [11] analyzed the effect of the blade pitch angle on the efficiency of a turbine for a VAWT. The results of CFD simulations indicate a clear dependence of the load distribution on the pitch angle, which gives greater possibilities for optimizing the efficiency of the wind turbine.

A good solution for small domestic installations in areas with low and time-varying wind velocity appears to be the application of vertical-axis wind turbines [12,13]. Small vertical-axis wind turbines can be an effective solution, especially for zero-energy buildings and urban models of distributed energy generation. Due to the significant dependence of turbine operation on wind velocity, a thorough environmental analysis is necessary when designing the installation, allowing the selection of an appropriate turbine construction and location. It is particularly crucial to include in the analysis the interactions between winds, buildings, and the topology of the urban area [14–17]. To improve the efficiency of wind turbines, they are most often placed on the roofs of buildings. This allows for reducing the interference related to turbulence caused by the interaction of the wind with the ground and buildings [18]. High turbulence intensity can result in lower energy production as well as higher mechanical stresses on the turbine components [19]. The Savonius turbine analyzed in the wind tunnel [20] showed that high-intensity turbulent flow affects the fluctuations of the loads acting on the turbine blades and consequently impacts the efficiency of the entire device. According to the measurements, for wind speeds below 7 m/s, the energy generated during high-intensity turbulent flow exceeded that obtained with a uniform flow of the same speed. After exceeding the certain velocity of wind, the energy generated for turbulent flow was significantly lower.

Efficiency can be improved by increasing airflow onto the wind turbine rotor. In the literature, several methods can be found to increase airflow, for example, by using "diffuser augmentation". A diffuser-augmented wind turbine (DAWT) has a diffuser installed downstream of the blades or a concentrator upstream to increase the flow speed acting on the blades [3]. There are many ducted or shrouded solutions for wind power applications, especially for small systems for individual users. This interest is mainly related to the

fact that such wind turbines can be significantly more efficient than similar rotors under free-flow conditions [21]. The subject of many studies [22–25] was to analyze the use of additional elements to increase the velocity of the air acting on the rotor, typically in the form of diffusers or concentrators. Bontempo et al. [26] presented a numerical analysis of the rotor enclosed in a profiled shroud. The authors noted that although an additional shroud for an existing turbine increases the turbine efficiency, significantly higher gains can be achieved by designing both the blades and the housing simultaneously to adapt the rotor geometry to the flow characteristics. In the study by Sridhar et al. [27], the authors analyzed the effect of diffuser geometric parameters, including the presence of slits and bleed air holes (the slotted DAWT). Their study showed that both slotted and non-slotted DAWTs obtained higher efficiency than the open wind turbine. Additionally, the slotted diffuser allowed for a 31% increase in air velocity compared to the full casing. Bontempo et al. [28] presents an approach to evaluating the performance of an optimal Joukowsky (free-vortex) rotor enclosed in a duct of general shape. Refaie et al. [29] studied an augmented horizontal-axis wind turbine. The authors analyzed the performance of the wind turbine through numerical investigation and an Archimedes-spiral wind turbine was selected as a test case. The main aim was to specify the optimal design, including additional concentrators, and therefore, to obtain the best performance of wind turbines for urban areas. Teklemariyem et al. [30] investigated the optimization of the geometry of the diffuser to increase airflow through the HAWT rotor. The analysis included different cross-sectional shapes, variable diffuser angles, and the presence of a flange. The obtained results allowed for the selection of a diffuser that would allow for the highest inflow velocity. Similar research was carried out by Shambira et al. [31]. The authors developed a diffuser design optimization model in the context of selecting the most appropriate geometric dimensions to achieve the highest flow velocity. Among the geometric parameters analyzed, in addition to the lengths of individual sections of the concentrator–throat–diffuser set, the diffuser and concentrator angles and flange height were also included. Based on the statistical analysis, it was noted that the concentrator length and diffuser length turned out to be the factors with the greatest influence, resulting in the highest increasing velocity.

This paper focuses on the influence of the design of a small wind turbine on energy efficiency. Among the parameters studied, both the shape and inclination of the rotor blades as well as the use of additional wind-concentrating elements were analyzed. The work was divided into two stages. In the first stage, experimental tests of different blade shapes on the achieved efficiency of the wind turbine were carried out. The angle of the blade was also taken into account during the measurements. In the next step, the influence of the additional aerodynamic shield on the air velocity flowing onto the turbine rotor was analyzed.

2. Materials and Methods

Commercial wind turbines are currently made mostly with a horizontal axis of rotation. One of the main limitations in domestic applications is the low wind speed. HAWTs are characterized by a higher power coefficient C_p but require higher wind speeds than VAWTs. Due to the small amount of data for horizontal-axis wind turbines of small diameter and operation at low wind speeds, the research in this article was focused on such an object.

The basic practical parameter that characterizes a wind turbine, crucial for potential users, is the electrical power that can be generated. Available turbines, especially for individual use, differ significantly in construction, number, as well as the shape of the blades. The experimental study carried out concentrates on measurements of the power generated by wind turbines and includes the effect of the shape of their blades and their inclination on the power and, as a consequence, on obtained wind turbine performance. With the development of computational fluid dynamics (CFD), numerical studies of wind turbines have become increasingly popular and attractive. Simulation studies involve a lower cost than experimental measurements in a wind tunnel. Numerical analyses are used to develop the optimal blade shape and also to determine the performance of the entire

turbine. An interesting issue analyzed using CFD is the impact of additional elements on turbine performance. The numerical analyses described in this article concentrate on evaluating the possibility of increasing the velocity of air coming over the turbine blades. The possibility to increase air velocity is extremely attractive from a wind turbine power perspective. As can be seen in the formula (Equation (1)) for the amount of power generated by a wind turbine, air velocity is one of the most important factors affecting power output because it appears in the formula at the third power. The research presented in this paper is divided into two parts, as described in the previous chapter.

2.1. Experimental Set-Up and Methodology

A research study has been carried out for horizontal-axis wind turbines with a diameter of up to 2 m. The laboratory tests were constructed to determine key turbine parameters under various conditions. The first step of testing consisted of determining the power generated by four different wind turbines, which differ in shape and also in the number of their blades. The second step of testing was performed only for the wind turbine characterized by having the best results from the first step of the evaluation, and this was intended to estimate the effect of the angle of attack of the turbine blades on its basic performance parameters. For the purpose of determining the effect of the angle of attack of the turbine blades, each of the turbine blades was individually rotated using plastic wedges. Wedges with different angles were used in the tests. During the laboratory tests, the turbine's rotational speed and the power generated by the turbines were measured in detail. All tests were carried out at constant wind speed and for various electrical loads of wind turbine generators. Measurements were performed for an air velocity equal to 8 m/s and the maximum rotational speed of the turbine rotor equal to 450 RPM. During the laboratory test, the electrical load was connected to the turbine's electrical generator and its value was set up during the measurements. The laboratory test stand was equipped, among other things, with an inverter-controlled set of 9 fans that were able to simulate wind velocity at the required level of magnitude and profile, as well as with a programming DC electronic load connected to the turbine electric generator RND 320-KEL103. Figure 2 shows the laboratory test stand including the above-described elements.

(**a**) (**b**) (**c**)

Figure 2. The laboratory stand: (**a**) fans' array simulating wind; (**b**) programming DC electronic load; and (**c**) plastic wedge to change blade inclination.

The shape of the turbine blades used in the study is shown in Figure 3.

Figure 3. Rotor turbine blades with different shapes: (**a**) BL1; (**b**) BL2; (**c**) BL3; and (**d**) BL4.

The first type of turbine, indicated as BL1, was characterized by blades with the largest chord, and the rotor used in this test consisted of 5 blades. The results for the second turbine were labeled BL2. This turbine was characterized by three blades and the second-largest chord of the tested blades. The rotors composed of BL3- and BL4-shaped blades were measured as five-bladed wind turbines, with the blades of the BL3 turbine having the smallest chord of all those tested.

2.2. Numerical Simulation Methodology

Numerical analyses were carried out to evaluate the velocity of incoming air in the cross-section of a wind turbine blade assembly. Simulations were carried out with Ansys Fluent 2020 R2 [32,33]. Analyses were performed for different shapes of aerodynamic shields added to the wind turbine constructions. It should be noted that a restriction was applied to the analyzed variants of the elements. The entire assembled system could not extend beyond a cube with a side length of 2000 mm. An additional assumption was that the device must be prepared so that the turbine rotor can be mounted inside a ring with a diameter as large as possible, i.e., of 1950 mm. Due to construction limitations, the length of the ring should be equal to 300 mm, thereby the total length of the aerodynamic shield (confusor or diffuser) can be maximally 1700 mm.

The CFD analyses were performed to verify the effect of the application of additional aerodynamic elements like a confusor or diffuser on the incoming air velocity to the rotor section at a constant wind speed equal to 3.0 m/s. The performed numerical analyses can be divided into two steps. The first step focuses on comparing the obtained velocities in the plane of a hypothetical wind turbine rotor using circle-to-circle and circle-to-square transitions in the diffuser or confusor versions. Figure 4 presents the geometries used in the numerical simulation.

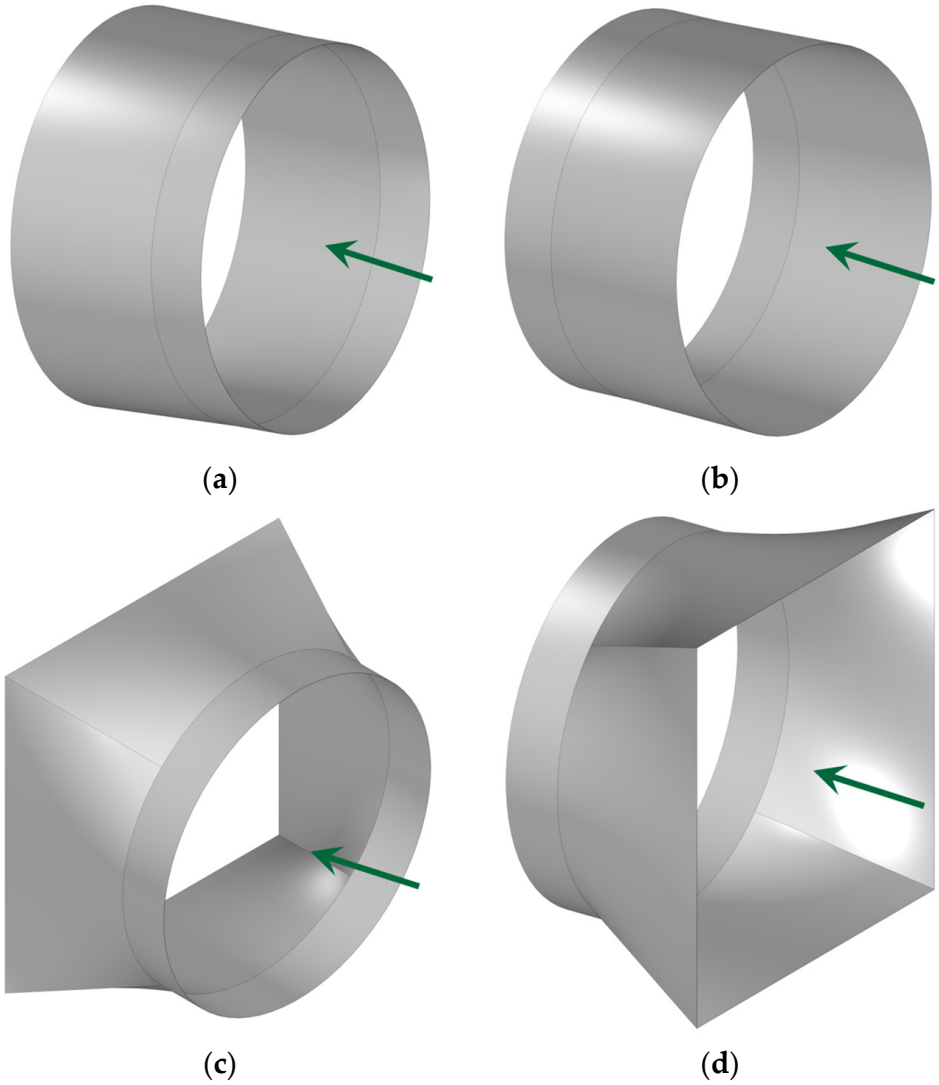

Figure 4. The geometry of the aerodynamic shield with: (**a**) increasing cross-sectional area (diffuser), circle to circle; (**b**) decreasing cross-sectional area (confusor), circle to circle; (**c**) increasing cross-sectional area (diffuser), square to circle; and (**d**) decreasing cross-sectional area (confusor), circle to square. The green arrow indicates the wind direction.

The analyses were carried out for five different lengths of these elements, by the reduction in the confusor or the diffuser length in the analyses. At the first step of the analysis, numerical simulations were used to estimate which one circle–circle or circle–square transition allows higher air velocities just before the rotor section. The second step consisted of evaluating the velocity of incoming air but with the confusor–diffuser configuration integrated into the more favorable version based on the analysis from the first step.

To perform numerical simulations, it is necessary to first prepare a computational model. The model set-up can be divided into three steps. The first step includes preparation of the geometry of the component under analysis and the surrounding environment. The next step is to generate mesh. The final step is the implementation of the required equations to perform calculations and analyze the results. Figure 5 presents the workflow for the simulation of the aforementioned problem, with all key steps highlighted.

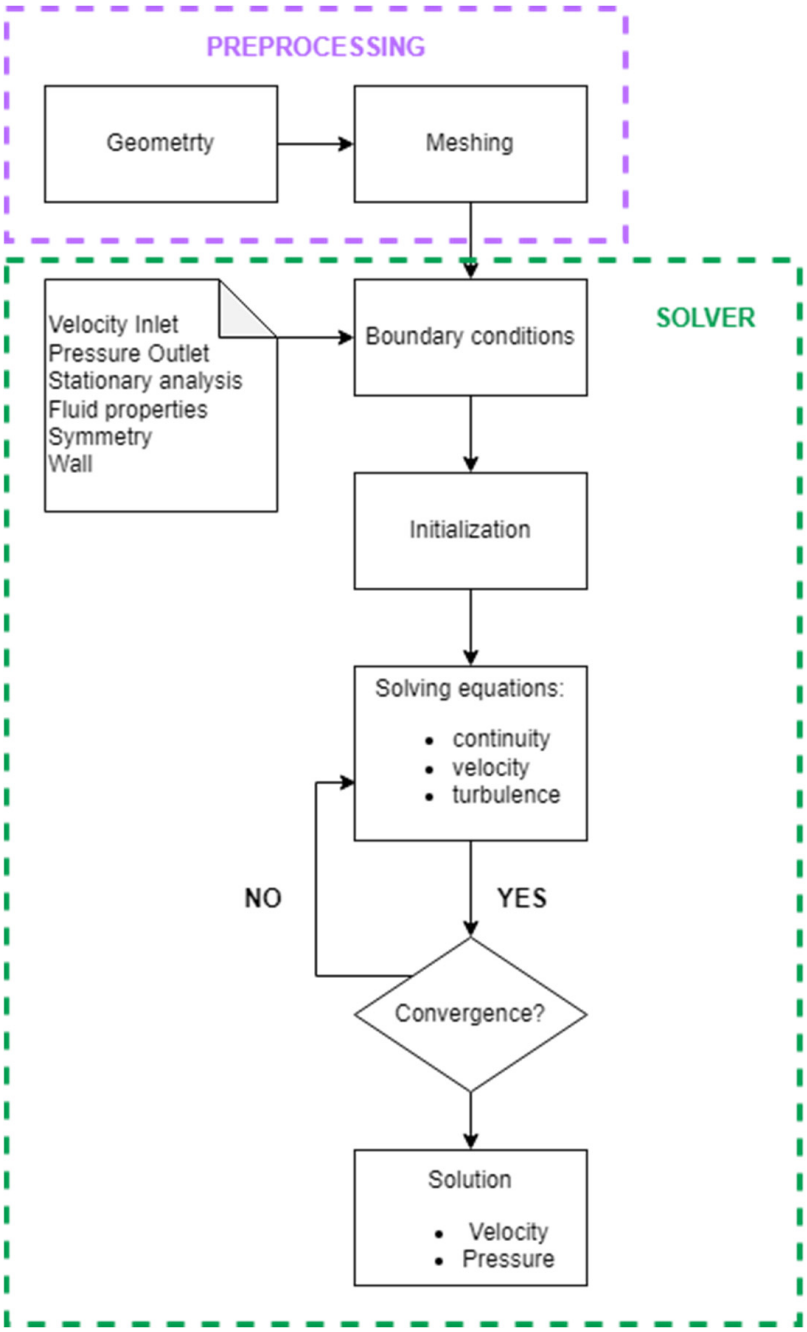

Figure 5. Block scheme of the workflow used for the simulation of the ducts.

To carry out the analyses, 3D models of the geometries were developed; due to their symmetries (geometrical symmetries and boundary condition symmetries), calculations were performed for one-quarter of the model geometry using the symmetry plane—see Figure 6a. The polyhexcore meshes were applied for the analyzed domain [34]—see Figure 6b,c.

In order to properly capture the boundary layer flow, the mesh was refined close to the walls using 20 inflation layers near the walls (first layer thickness set as 0.00015 m with growth ratio 0.272). For all tested cases, the dimensionless wall distance y+ does not exceed 5. Mesh refinement was also applied to the volume around the test element. The test case used a mesh with a size of 600.000 elements. The settings and size of the mesh were selected based on the comparison with two other configurations with a higher number of control volumes, at 1.3 million and 2.4 million, respectively. The difference in average air velocity

was approx. ±0.2% for both cases. Additional refinement with the element size of 0.04 m was applied around the walls of the structure to capture the vortex behavior as well as avoid rapid changes in mesh size through the domain.

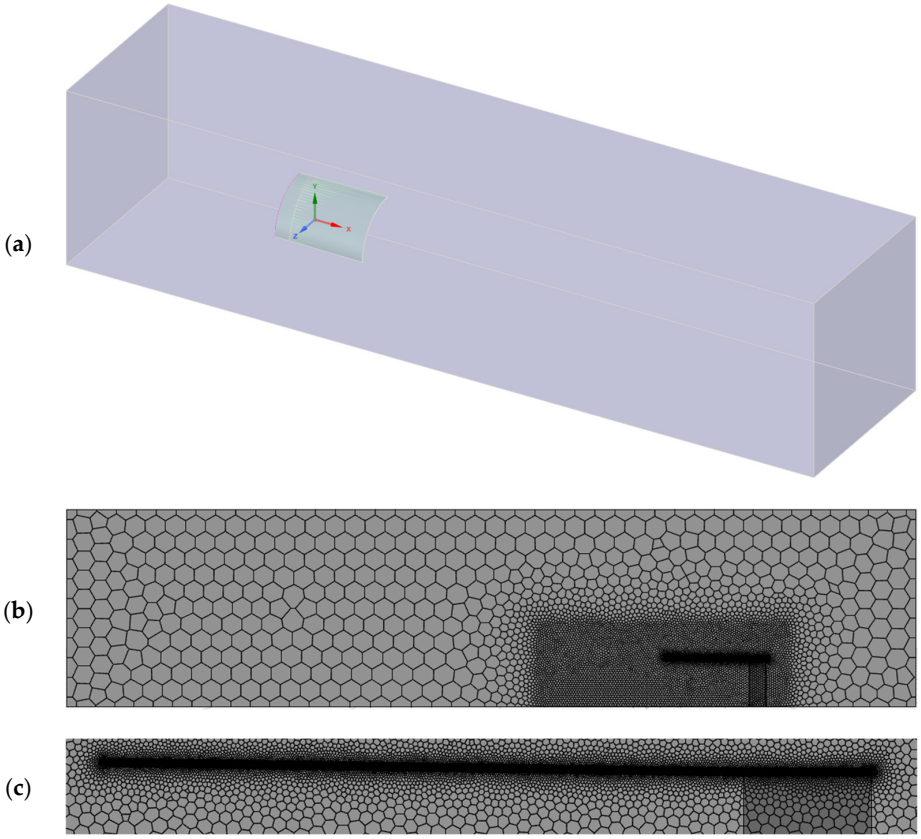

Figure 6. Computational domain: (**a**) geometry; (**b**) mesh—the entire computational domain; and (**c**) mesh—an increase in local mesh density around the wall of the aerodynamic shield.

The k-ω SST turbulence model was used in the simulation [35]. The k-ω SST model is a model that combines the advantages of the k-ε model and the k-ω model. The k-ε model resolves the turbulent flow properly in free flow and the shear layers well and is characterized by low sensitivity to the inlet conditions for quantities describing turbulence. The k-ω model, on the other hand, resolves turbulent flow structures in the boundary layer much better than the k-ε model. The calculation uses a cuboid as the computational domain. At the entrance to the computational domain, the "velocity inlet" boundary condition was used with a constant value equal to 3.0 m/s. The "pressure outlet" boundary condition was applied at the domain exit. For both inlet and outlet, the turbulence intensity was set to 5% and the viscosity ratio to 10. The symmetry condition on the side walls of the domain was used. No-slip boundary conditions were applied on the walls. The pressure-based solver and SIMPLE algorithm were applied. The discretization schemes used for calculation were second-order upwind schemes and for gradient least squares, cell based.

3. Results

3.1. Effect of the Blade Shape and Inclination Angle—Experimental Results

The performance of the small wind turbine with different blade shapes and different numbers of blades was analyzed. Based on the laboratory measurement results, Figure 7 was plotted. It represents the wind turbine power P as a function of the turbine rotational speed.

As the rotational speed increased, the power output increased for all of the tested wind turbines. Once the turning point was reached, the power output began to decrease.

For almost all rotational speeds, the highest values of the power output P were obtained for the five-bladed wind turbine with the largest chord, labeled as BL1. The results obtained for the turbine composed of blade types BL3 or BL4 were very similar, especially for higher rotational speeds, and simultaneously lower than for the turbine composed of blades labeled BL2. The maximum power was achieved at around 350 RPM for all tested configurations. Comparing the values obtained for the individual turbines at this rotational speed, the BL2 turbine produced about 5% less power than the BL1 turbine, the BL3 turbine about 26%, and the BL4 turbine about 35% less power than the BL1 turbine. For a rotational speed of around 400 RPM, the wind turbine with blades labeled BL2 obtained slightly higher performance than the BL1 turbine. The wind turbine with blades BL2 generated approx. 8% higher power than BL1 at this rotational speed, while the BL3 wind turbine had approx. 35% and the BL4 turbine approx. 40% lower power than the five-blade BL1 wind turbine.

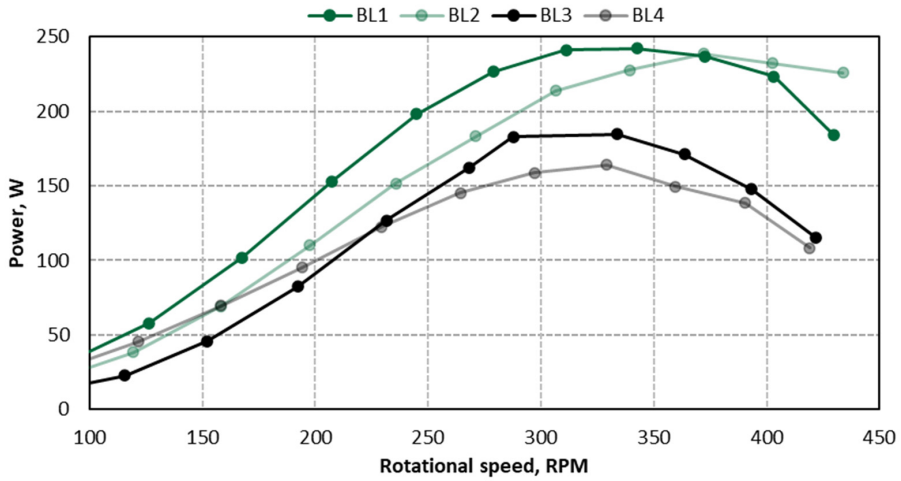

Figure 7. The power output *P* of the wind turbine as a function of the turbine rotational speed.

Based on the analysis presented above, to evaluate the effect of the blades' inclination angle on the wind turbine power output, a turbine with five blades of the BL1 type was selected. Tests were carried out for no blade inclination (0°) and tilt angles of +3°; +6° (clockwise) as well as −3°, and −6° (counterclockwise), respectively. Figure 8 shows the wind turbine's power output as a function of the turbine rotational speed for the tested inclination angles of the blades BL1.

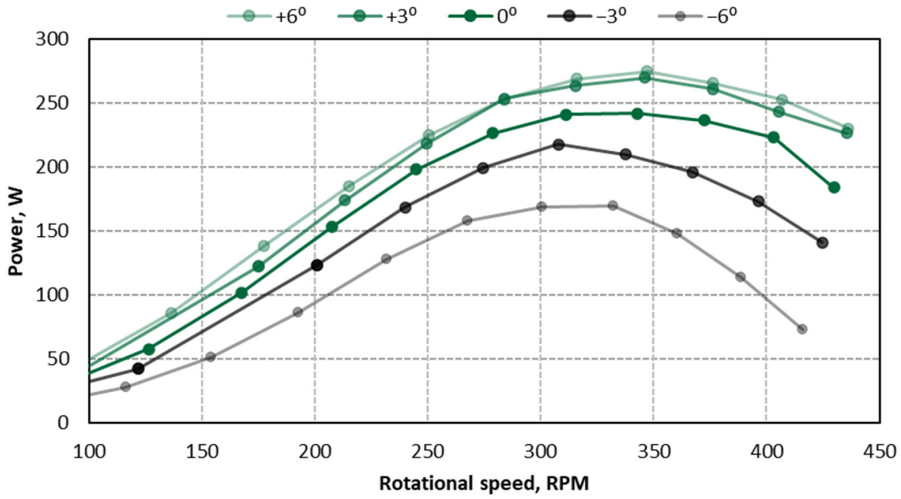

Figure 8. The power output *P* of the wind turbine as a function of the turbine rotational speed for various inclination angles of wind turbine blades BL1.

It has been found that modification in the inclination angle of the blades in the wind turbine had a significant effect on the power output. By comparing Figures 7 and 8, it is apparent that the BL1 inclination angles of the blades could influence the output power of the turbine more significantly than the shape of the blade. During the analysis, it was evaluated that the highest power outputs were achieved with the blades set at the "+" clockwise angle of attack. For the measurements carried out, the highest power output was obtained for the +6° angle of attack, which resulted in a 16% increase in peak power compared to blades at the base setting and a 66% increase in comparison to blades with the angle of −6°.

3.2. Effect of the Aerodynamic Shield on the Air Velocity in the Rotor Section—Numerical Simulation Results

With numerical research, it is possible to develop a geometry of the aerodynamic shield and assess its ability to increase the average velocity in the rotor cross-sectional plane. As presented in the section describing the research methodology, the numerical analyses began with a comparison of different types of shields dedicated as accessories to wind turbines. In the first stage, the velocity distributions inside and around the aerodynamical shield were compared for four shapes of elements, i.e., two diffusers (circle–circle and circle–square) and two confusors (also circle–circle and circle–square). The results are presented in Figure 9, which contains the velocity distribution in the symmetry plane of the shield for each of the analyzed types of elements for the length L = 666 mm. All drawings were prepared for a common velocity scale.

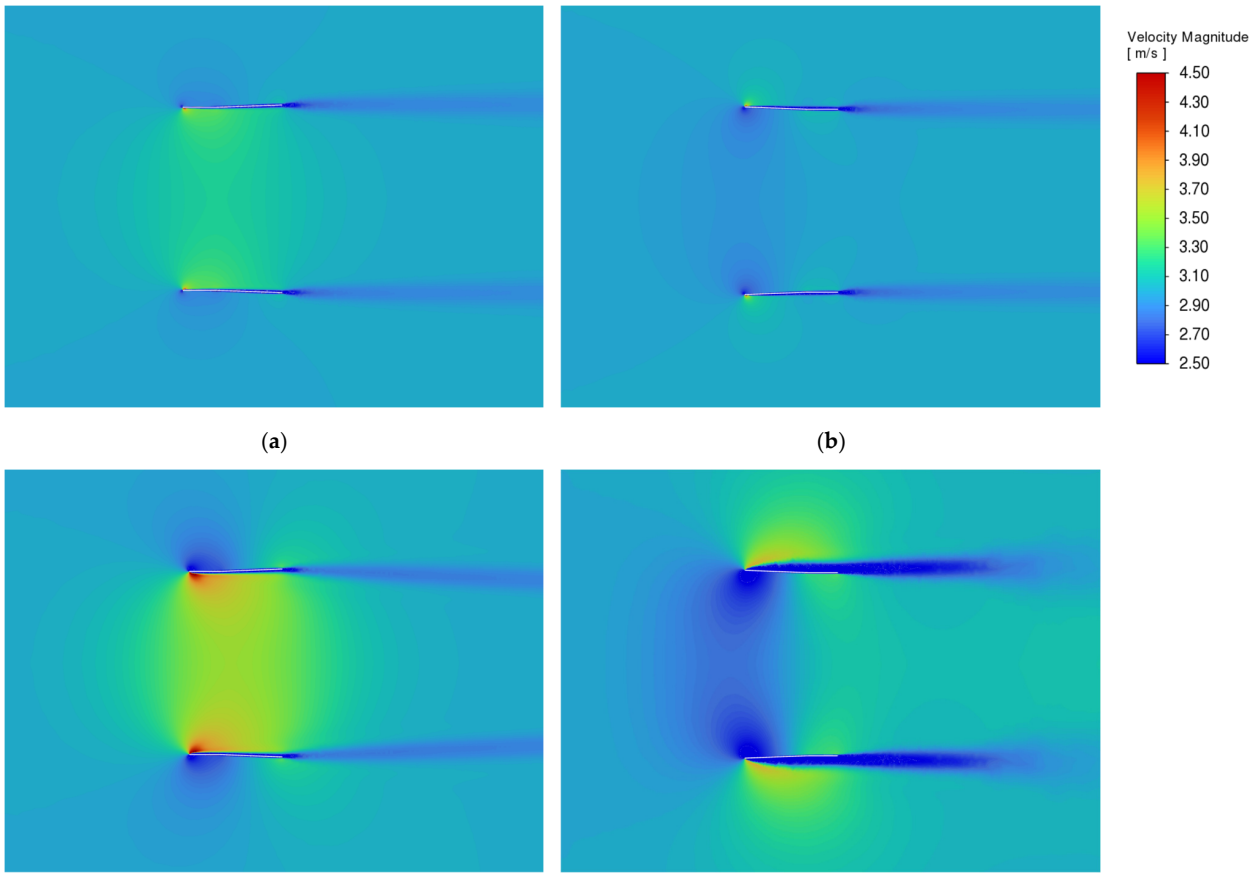

Figure 9. Velocity distribution inside and around the shield for the following configurations: (**a**) diffuser circle-to-circle; (**b**) confusor circle-to-circle; (**c**) diffuser square-to-circle; and (**d**) confusor circle-to-square.

When comparing the velocity distribution in the analyzed configurations, it should be noted that the most important aspect is the velocity in the rotor section. It should be emphasized that in the case of diffusers, this is the section at the beginning of the aerodynamic shield, while in the case of the confusor, it is at its end. As can be seen, for both variable and constant cross-sectional shapes, the diffuser configurations allow for obtaining significantly higher velocity values in the rotor section than the confusor variants. The results for circle-to-circle shapes (Figure 9a,b) show that the flow is more even and without accumulations or local increases in velocity. Changing the shapes, on the other hand, causes local accumulation, and thus a more uneven velocity distribution in the inlet section. Analyzing Figure 9c, i.e., the square-to-circle diffuser, the highest velocities are visible locally at the shield walls. The values there are noticeably higher than any other presented variants. In turn, analyzing Figure 9d, one can observe a low velocity at the inlet of the circle-to-square confusor, also resulting from a much larger cross-section of the cover. However, looking at the rotor sections, an increase in the flow velocity and a fairly uniform flow is visible.

Analogous analyses were performed for other shield lengths. The obtained results can be plotted as a function of the length of the diffuser/confusor in the circle-to-circle and circle-to-square configurations of the aerodynamic shield set-up (see Figure 10).

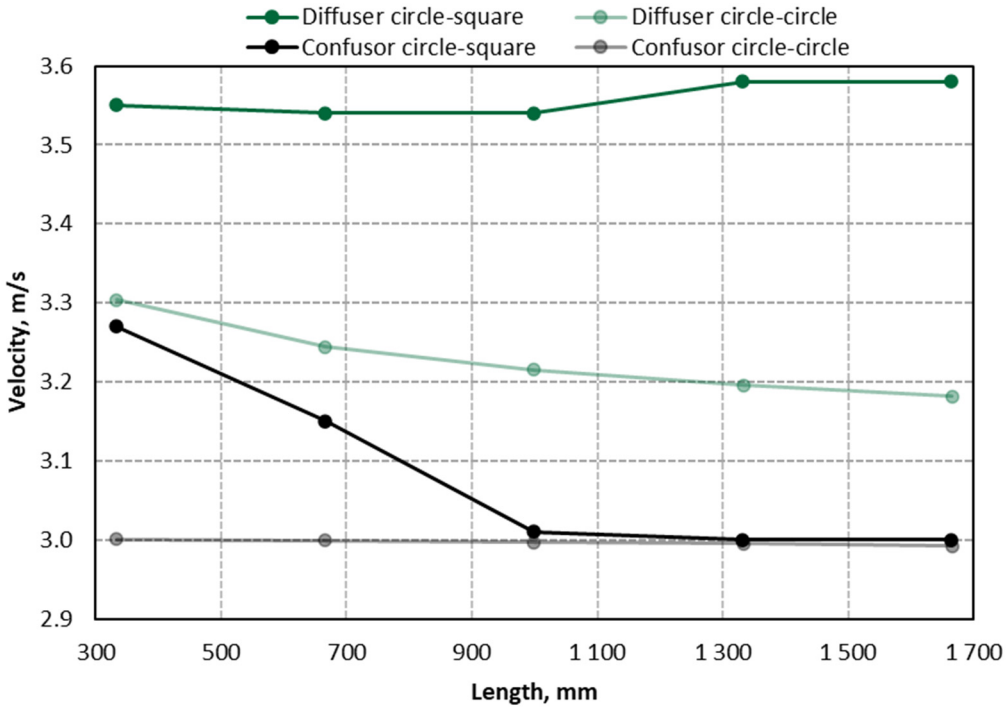

Figure 10. Velocity in a cross section as a function of the diffuser and confusor lengths in the circle-to-circle and circle-to-square configurations.

For the circle-to-square diffuser configuration, increasing the length of this element increases the air velocity in the rotor plane section. For the longest version of the diffuser analyzed, a 1% increase in velocity was obtained compared to that of the diffuser with the smallest length. As can be seen, the increase, although it occurred, is very small. For the circle-to-circle diffuser configuration and both confusors, an increase in their length results in a decrease in air velocity. The velocity reduction of 8% for the confusor circle-to-square configuration, 4% for the diffuser circle-to-circle configuration, and less than 0.5% for the confusor circle-to-circle configuration was observed, respectively. Furthermore, as can be seen in Figure 10, for the diffuser circle-to-square configuration, a higher velocity of 8% was achieved than for the diffuser circle-to-circle configuration. Simultaneously, for the diffuser circle-to-square configuration, it was possible to obtain approximately an 8% higher velocity

than for the diffuser circle-to-circle configuration. For the circle-to-circle configuration, the aerodynamic shield gives lower air velocity values than the circle-to-square variant. These correlations are evident for both the confusor and the diffuser.

The conclusions drawn from the above analysis allowed for the assumption that a combination of these two elements can be a good solution to increase the air velocity in the rotor section of a wind turbine. The set consisted of a module with a decreasing cross-section (confusor) at the inlet, the rotor section, and a module with an increasing cross-section (diffuser) behind it. Since significantly better results were achieved for the circle-to-square cross-section, further analysis was conducted for a combined confusor and diffuser system in the circle-square version. Figure 11 presents an example of geometry used in the numerical simulation.

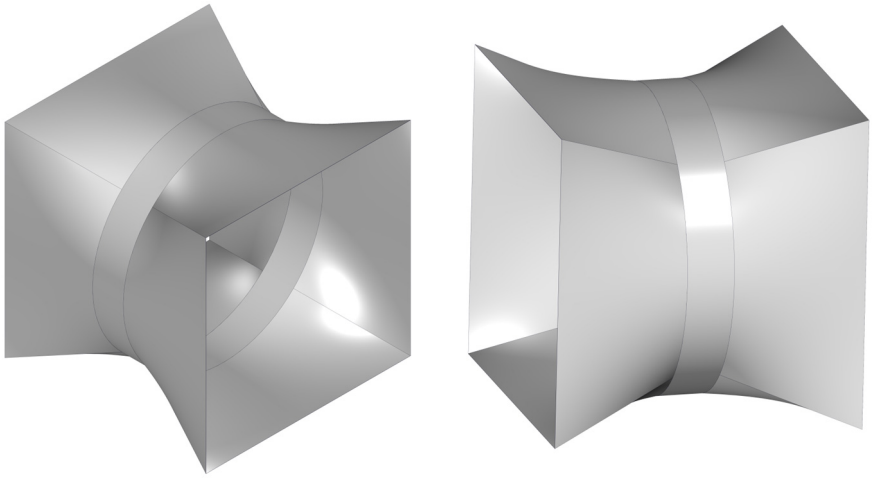

Figure 11. The geometry of the confusor–diffuser configuration used in the numerical simulation.

The calculations performed included various variants differing in the length of individual sections. The analysis was carried out assuming that the total length of the tested system should be 1966 mm. This length already includes the circular ring with a length of 300 mm, which is designed for the rotor. The study focused on four variants with different lengths of the components. The details of the selected variants subject to analysis are presented in Figure 12.

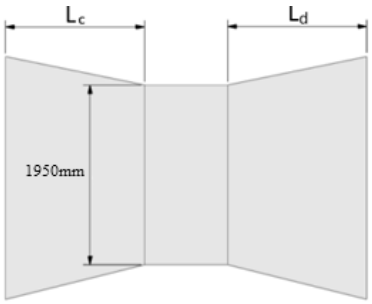

Configuration	CD_1	CD_2	CD_3	CD_4
L_c, mm	111	222	333	833
L_d, mm	1555	1444	1333	833
L_{c+d}, mm	1666	1666	1666	1666
L_{total}, mm	1966	1966	1966	1966

Figure 12. Framework of different variants for the lengths of combined diffuser and confusor elements.

For each of the variants, a geometric model was prepared, which then constituted the basis for the meshing process and numerical calculations. The assumptions and settings adopted were consistent with those used at the analysis stage of the individual elements (diffusers and confusors). Based on the CFD results, the average incoming air velocity into the rotor section of the wind turbine was analyzed. The summary of the values obtained is presented in Figure 13.

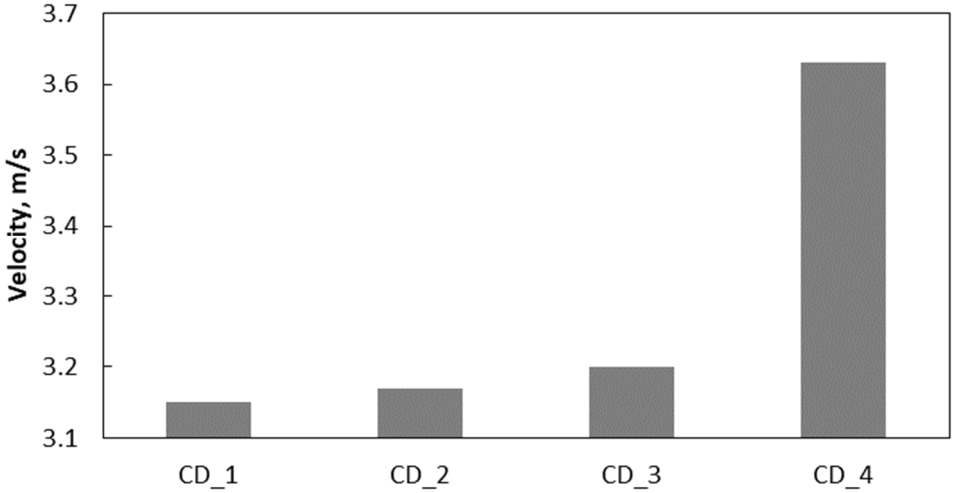

Figure 13. The average velocity in the rotor cross-section for the tested confusor–diffuser (CD) sets (according to Figure 12).

For the configuration labeled CD_4, the air velocity in the analyzed section was the highest. For the longest length of the confusor in the combined confusor and diffuser system, a 13% increase in velocity was obtained compared to the combined confusor and diffuser system with the smallest length of the confusor (CD_1). Lengthening the diffuser part of the combined set increased the velocity at the rotor cross-section. The highest increase in air velocity occurred when the lengths of the confusor and diffuser were the same. The results for configuration that allow for the highest velocity in the rotor section, i.e., CD_4, will be presented in detail below. Figure 14 shows the velocity distribution inside and around the aerodynamic shield CD_4. Figure 14a presents pathlines in the 3D view of the model. The velocity field and velocity vector distribution in the plane of the longitudinal section of the tested element are presented in Figures 14b and 14c, respectively.

As can be seen, the higher velocities are obtained in the middle of the distance between the inlet and outlet of the shield, i.e., in the rotor section. An increase in local velocities closer to the shield walls is also visible. Flow analysis, similar to the example presented, was performed for each configuration included in the research. On this basis, it was possible to assess the flow characteristics and the potential in the context of increasing the speed in the rotor section.

(**a**)

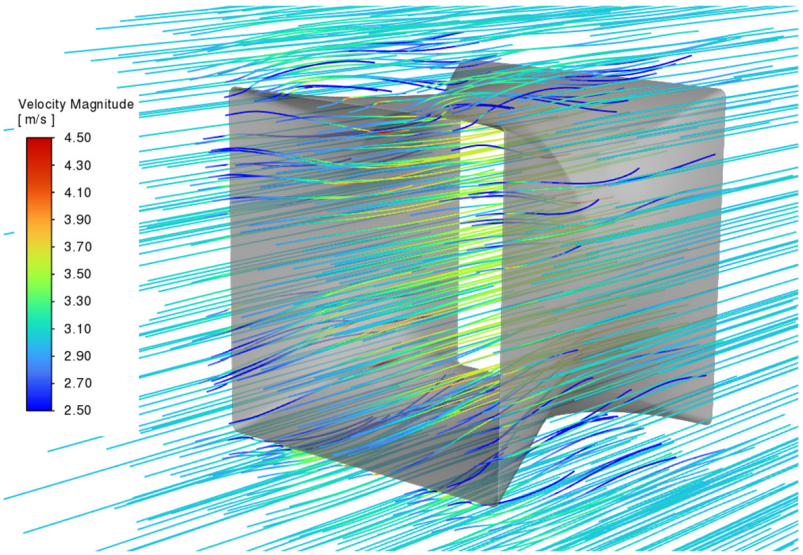

Figure 14. *Cont.*

(**b**)

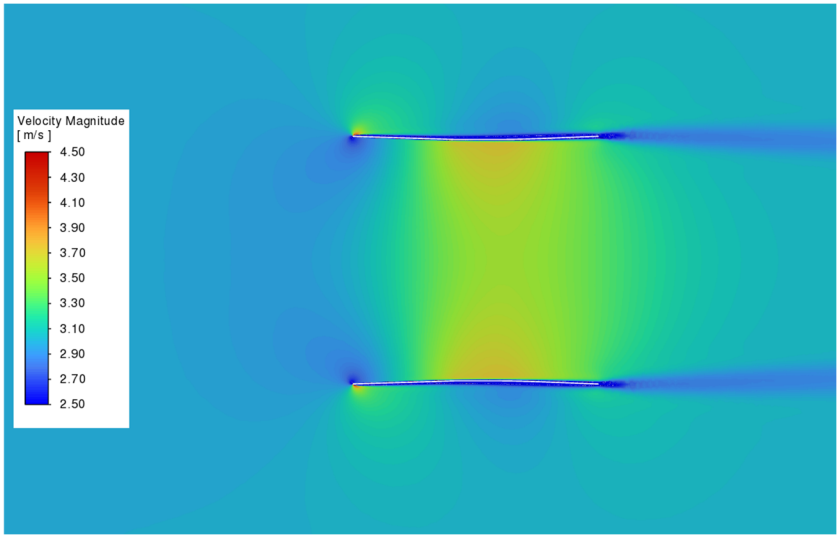

(**c**)

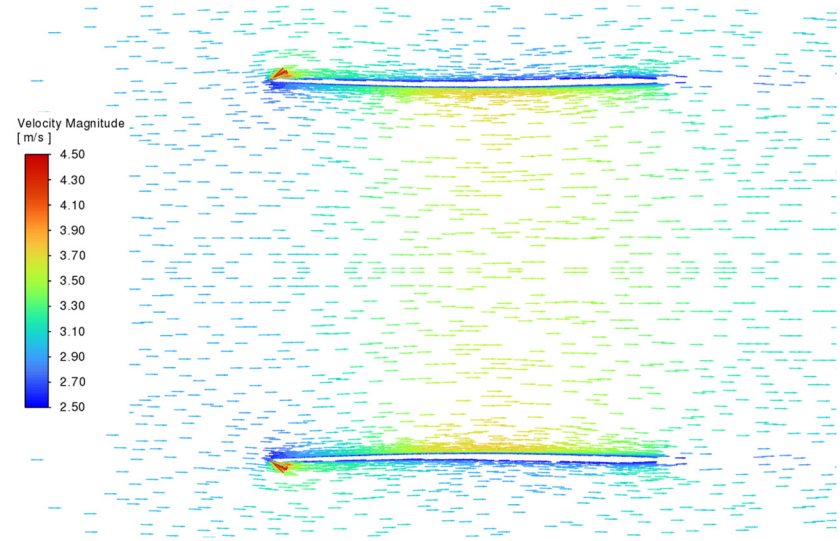

Figure 14. Air velocity inside and around a condenser–diffuser shield CD_4: (**a**) pathlines; (**b**) velocity field; and (**c**) velocity vectors.

To summarize, for a combined system of a confusor and a diffuser with the same length of 833 mm (configuration CD_4), a velocity in the rotor cross-section increases up to approximately 3.63 m/s. For the combined confusor and diffuser system, this translates into a significant air velocity increase of about 21% compared to the incoming air velocity.

4. Discussions

The results of the experimental studies provide important information on the influence of the blade shape and pitch angle on the efficiency of wind turbines. Additionally, numerical simulations allowed us to assess the effectiveness of using additional aerodynamic shields, such as diffusers/confusors, to increase the air velocity flowing through the turbine blades.

4.1. Effect of the Blade Shape and Inclination Angle

The analysis of the experimental results clearly shows that the shape of the blades and the number of blades have a significant influence on the efficiency of the wind turbine. Among the tested configurations, the turbine equipped with five blades with the largest chord (BL1) generated the highest power at almost all rotational speeds. Compared with other configurations, the differences in performance were clear—BL1 obtained about 5%

more power than BL2, 26% more than BL3, and as much as 35% more than BL4. These results show that the appropriate shape of the blades and their number can lead to the improved efficiency of wind turbines.

Another important factor influencing turbine performance was the blade pitch angle. Changing the blade pitch angle of the BL1 blades had a clear effect on the turbine output power. The best results were achieved at an angle of +6° (clockwise), which resulted in a power increase of 16% compared to the blades set in the initial position and 66% compared to the blades set at −6°. These results indicate that optimizing the blade pitch angle can significantly improve the performance of wind turbines, even more than modifying the blade shape itself.

4.2. Effect of the Aerodynamic Shield on the Air Velocity in the Rotor Section

Numerical simulations carried out for different aerodynamic shield configurations showed that the use of properly designed diffusers and confusors can significantly affect the air velocity entering the turbine blade section. The results showed that for the diffuser configuration with a circle-to-square transition, extending its length leads to an increase in the air velocity in the rotor plane. The greatest increase in speed, by about 13%, was achieved with the longest version of the confusor combined with a diffuser of the same length. Based on this research, it can be concluded that appropriate optimization of the length and shape of aerodynamic shields can significantly improve the efficiency of wind turbines by increasing the speed of air reaching the blades, which directly translates into greater power generated by the turbine.

5. Conclusions

In this paper, the impact of the design parameters on the power output of a small wind turbine has been analyzed experimentally and using numerical modeling. The shape of the rotor blades and inclination of the rotor blades as well as the use of additional aerodynamic shields were analyzed.

The analysis indicates that the power output of the wind turbine is strongly influenced by the type of blade and the angle of the blades' inclination. The study showed that the best results were obtained by the turbine with blades labeled as BL1. At the same time, the power output for each type of blade depends on the rotational speed. Comparing the values obtained for the individual turbines at a rotational speed of 350 RPM (for most of the tested rotors the maximum power output was achieved around this value), the wind turbines generated approximately 5% to 35% less power, depending on the type of wind turbine blades. The results also indicate the importance of the inclination angle of wind turbine blades. By changing the angle of inclination, up to a 16% increase in power generated by the wind turbine under study was achieved.

The power output of the wind turbine is highly dependent on the wind velocity, as can be deduced by a well-known formula (Equation (1)). Even a small increase in wind velocity can result in significant growth in electrical power. The presented results show that the optimized combined confusor and diffuser set allows for increasing the incoming air velocity on the rotor section. Adequate aerodynamic shapes make wind turbines more efficient and perform better. In the analyzed configuration, an approximate 21% increase in wind speed was observed, resulting in an increase of 77% in wind turbine power output (assuming a constant C_p coefficient).

Author Contributions: Conceptualization, J.H. and K.Z.-G.; methodology, J.H.; software, P.M.; validation, J.H., K.Z.-G. and P.M.; formal analysis, K.Z.-G.; investigation, J.H.; resources, P.M.; data curation, M.J.; writing—original draft preparation, K.Z.-G.; writing—review and editing, M.J. and M.B.; visualization, J.H.; supervision, M.B.; project administration, M.J.; funding acquisition, M.B. All authors have read and agreed to the published version of the manuscript.

Funding: This article was supported by the program "Excellence initiative—research university" for the AGH University of Krakow.

Data Availability Statement: The raw data supporting the conclusions of this article will be made available by the authors on request.

Conflicts of Interest: The authors declare no conflicts of interest.

References

1. Schaffarczyk, A.P. *Introduction to Wind Turbine Aerodynamics*, 3rd ed.; Springer Nature: Cham, Switzerland, 2024.
2. Kalmikov, A. Wind power fundamentals. In *Wind Energy Engineering. A Handbook for Onshore and Offshore Wind Turbines*, 2nd ed.; Letcher, T.M., Ed.; Academic Press: London, UK, 2023.
3. Wood, D. *Small Wind Turbines: Analysis, Design, and Application*; Springer: Berlin/Heidelberg, Germany, 2011.
4. Wolniewicz, K.; Kuczyński, W.; Zagubień, A. *Evaluation of Wind Resources for Horizontal and Vertical Wind Turbine*; Monography of the Faculty of Mechanical Engineering University of Technology: Koszalin, Poland, 2019.
5. James, P.A.B.; Bahaj, A.B.S. Small-scale wind turbines. In *Wind Energy Engineering. A Handbook for Onshore and Offshore Wind Turbines*, 2nd ed.; Letcher, T.M., Ed.; Academic Press: London, UK, 2023.
6. Benim, A.C.; Diederich, M.; Pfeiffelmann, B. Aerodynamic Optimization of Airfoil Profiles for Small Horizontal Axis Wind Turbines. *Computation* **2018**, *6*, 34. [CrossRef]
7. Muhsen, H.; Al-Kouz, W.; Khan, W. Small Wind Turbine Blade Design and Optimization. *Symmetry* **2020**, *12*, 18. [CrossRef]
8. Deghoum, K.; Gherbi, M.T.; Sultan, H.S.; Jameel Al-Tamimi, A.N.; Abed, A.M.; Abdullah, O.I.; Mechakra, H.; Boukhari, A. Optimization of Small Horizontal Axis Wind Turbines Based on Aerodynamic, Steady-State, and Dynamic Analyses. *Appl. Syst. Innov.* **2023**, *6*, 33. [CrossRef]
9. Umar, D.A.; Yaw, C.T.; Koh, S.P.; Tiong, S.K.; Alkahtani, A.A.; Yusaf, T. Design and Optimization of a Small-Scale Horizontal Axis Wind Turbine Blade for Energy Harvesting at Low Wind Profile Areas. *Energies* **2022**, *15*, 3033. [CrossRef]
10. Shen, X.; Yang, H.; Chen, J.; Zhu, X.; Du, Z. Aerodynamic shape optimization of non-straight small wind turbine blades. *Energy Convers. Manag.* **2016**, *119*, 266–278. [CrossRef]
11. Rezaeiha, A.; Kalkman, I.; Blocken, B. Effect of pitch angle on power performance and aerodynamics of a vertical axis wind turbine. *Appl. Energy* **2017**, *197*, 132–150. [CrossRef]
12. Dinh Le, A.; Nguyen Thi Thu, P.; Ha Doan, V.; The Tran, H.; Duc Banh, M.; Truong, V.-T. Enhancement of aerodynamic performance of Savonius wind turbine with airfoil-shaped blade for the urban application. *Energy Convers. Manag.* **2024**, *310*, 118469. [CrossRef]
13. Xu, W.; Li, G.; Zheng, X.; Li, Y.; Li, S.; Zhang, C.; Wang, F. High-resolution numerical simulation of the performance of vertical axis wind turbines in urban area: Part I, wind turbines on the side of single building. *Renew. Energy* **2021**, *177*, 461–474. [CrossRef]
14. Ye, X.; Zhang, X.; Weerasuriya, A.U.; Hang, J.; Zeng, L.; Li, C.Y. Optimum Design Parameters for a Venturi-Shaped Roof to Maximize the Performance of Building-Integrated Wind Turbines. *Appl. Energy* **2024**, *355*, 122311. [CrossRef]
15. Abdelsalam, A.M.; Abdelmordy, M.; Ibrahim, K.; Sakr, I. An investigation on flow behavior and performance of a wind turbine integrated within a building tunnel. *Energy* **2023**, *280*, 128153. [CrossRef]
16. Dilimulati, A.; Stathopoulos, T.; Paraschivoiu, M. Wind turbine designs for urban applications: A case study of shrouded diffuser casing for turbines. *J. Wind Eng. Ind. Aerodyn.* **2018**, *175*, 179–192. [CrossRef]
17. Mao, Z.; Yang, G.; Zhang, T.; Tian, W. Aerodynamic Performance Analysis of a Building-Integrated Savonius Turbine. *Energies* **2020**, *13*, 2636. [CrossRef]
18. Lee, K.-Y.; Tsao, S.-H.; Tzeng, C.-W.; Lin, H.-J. Influence of the vertical wind and wind direction on the power output of a small vertical-axis wind turbine installed on the rooftop of a building. *Appl. Energy* **2018**, *209*, 383–391. [CrossRef]
19. Riziotis, V.A.; Voutsinas, S.G. Fatigue loads on wind turbines of different control strategies operating in complex Terrain. *J. Wind Eng. Ind. Aerodyn.* **2000**, *85*, 211–240. [CrossRef]
20. Wekesa, D.W.; Wang, C.; Wei, Y.; Zhu, W. Experimental and numerical study of turbulence effect on aerodynamic performance of a small-scale vertical axis wind turbine. *J. Wind Eng. Ind. Aerodyn.* **2016**, *157*, 1–14. [CrossRef]
21. Jamieson, P. *Innovation in Wind Turbine Design*, 2nd ed.; Wiley: Hoboken, NJ, USA, 2018.
22. Masukume, P.-M.; Makaka, G.; Mukumba, P. Optimization of the Power Output of a Bare Wind Turbine by the Use of a Plain Conical Diffuser. *Sustainability* **2018**, *10*, 2647. [CrossRef]
23. Watanabe, K.; Ohya, Y.; Uchida, T. Power Output Enhancement of a Ducted Wind Turbine by Stabilizing Vortices around the Duct. *Energies* **2019**, *12*, 3171. [CrossRef]
24. Hwang, P.-W.; Wu, J.-H.; Chang, Y.-J. Optimization Based on Computational Fluid Dynamics and Machine Learning for the Performance of Diffuser-Augmented Wind Turbines with Inlet Shrouds. *Sustainability* **2024**, *16*, 3648. [CrossRef]
25. Alkhabbaz, A.; Yang, H.-S.; Tongphong, W.; Lee, Y.-H. Impact of compact diffuser shroud on wind turbine aerodynamic performance: CFD and experimental investigations. *Int. J. Mech. Sci.* **2022**, *216*, 106978. [CrossRef]
26. Bontempo, R.; Di Marzo, E.M.; Manna, M. Diffuser augmented wind turbines: A critical analysis of the design practice based on the ducting of an existing open rotor. *J. Wind Eng. Ind. Aerodyn.* **2023**, *238*, 105428. [CrossRef]
27. Sridhar, S.; Zuber, M.; Shenoy, S.B.; Kumar, A.; Ng, E.Y.K.; Radhakrishnan, J. Aerodynamic comparison of slotted and non-slotted diffuser casings for Diffuser Augmented Wind Turbines (DAWT). *Renew. Sustain. Energy Rev.* **2022**, *161*, 112316. [CrossRef]

28. Bontempo, R.; Manna, M. The Joukowsky rotor for diffuser augmented wind turbines: Design and analysis. *Energy Convers. Manag.* **2022**, *252*, 114952. [CrossRef]
29. Refaie, A.G.; Abdel Hameed, H.S.; Nawar, M.A.A.; Attai, Y.A.; Mohamed, M.H. Qualitative and quantitative assessments of an Archimedes Spiral Wind Turbine performance augmented by A concentrator. *Energy* **2021**, *231*, 121128. [CrossRef]
30. Teklemariyem, D.A.; Yimer, E.T.; Ancha, V.R.; Zeru, B.A. Parametric study of an empty diffuser geometric parameters and shape for a wind turbine using CFD analysis. *Heliyon* **2024**, *10*, e26782. [CrossRef] [PubMed]
31. Shambira, N.; Makaka, G.; Mukumba, P. Velocity Augmentation Model for an Empty Concentrator-Diffuser-Augmented Wind Turbine and Optimisation of Geometrical Parameters Using Surface Response Methodology. *Sustainability* **2024**, *16*, 1707. [CrossRef]
32. ANSYS. *Fluent Theory Guide*; Release 20.1; ANSYS, Inc.: Canonsburg, PA, USA, 2020. Available online: https://www.ansys.com/products/fluids/ansys-fluent (accessed on 30 April 2024).
33. Marczak, P. Design of a Building Integrated Wind Turbine. Master's Thesis, AGH University of Krakow, Kraków, Poland, 2021. (In Polish).
34. Zore, K.; Sasanapuri, B.; Parkhi, G.; Varghese, A. Ansys Mosaic Poly-Hexcore mesh for high-lift aircraft configuration. In Proceedings of the 21th Annual CFD Symposium, Bangalore, India, 8–9 August 2019.
35. Uchida, T.; Taniyama, Y.; Fukatani, Y.; Nakano, M.; Bai, Z.; Yoshida, T.; Inui, M. A New Wind Turbine CFD Modeling Method Based on a Porous Disk Approach for Practical Wind Farm Design. *Energies* **2020**, *13*, 3197. [CrossRef]